ELSEVIER

Thermochimica Acta 319 (1998) 123–129

thermochimica acta

Melting and recrystallization of a thermotropic liquid crystalline copolyester

G. Wiberg, U.W. Gedde*

Department of Polymer Technology, Royal Institute of Technology, S-100 44 Stockholm, Sweden

Received 26 July 1997; accepted 1 June 1998

Abstract

Oriented samples of a liquid crystalline polymer (Vectra A950) analyzed in direct contact with an aluminium pan shrunk and curled during heating in the DSC which led to a very noisy baseline and an artificial multimodal melting. Oriented samples immersed in silicone oil or surrounded by Kapton films were free to shrink, remained in good thermal contact with the aluminium pan and displayed noise-free heating thermograms with a single melting peak. The constrained samples showed noise free, unimodal melting in the 260–290°C range. Annealing of Vectra samples between 250 and 300°C led to a gradual increase in both the melting enthalpy and the melting peak temperature with increasing annealing time. Crystallization of the pure nematic polymer was facilitated by orientation. © 1998 Elsevier Science B.V.

Keywords: Crystallization; DSC; Liquid crystalline copolyester; Melting; Thermotropics

1. Introduction

Differential scanning calorimetry (DSC) is a widely used for determining various physical and chemical processes in polymers. The temperature and energy control enable high-precision determination of transition temperatures and enthalpies. A key to obtain reproducible results is that good physical contact is achieved between the sample and the sample pan. Any movement of the sample during the experiment will give rise to a noisy signal [1]. Nucleation of crystallization from the substrate (sample pan) interface may lead to erroneous results revealed as shoulders or additional peaks in the thermograms [2].

The melting and crystallization/recrystallization behaviour of thermotropic liquid crystalline copolyesters is complex and it is often very difficult to obtain reproducible thermograms. The melting transitions often involve very small enthalpies [3]. A previous study [3] dealing with orientation/relaxation effects in a copolyester based on hydroxybenzonic acid and hydroxynaphtoic acid (Vectra A950) subjected to various types of heat treatments demonstrated that the way the sample was clamped during the experiment was crucial for the outcome of the experiment. A distinction was made between freely shrinking samples which were able to change their dimensions during the heating scan which led to an almost instantaneous loss of global orientation above the crystal melting point, whereas samples held at constant length during the experiment increased their global orientation on heating.

This paper reports the effect of the degree of orientation on the melting/recrystallization behaviour of Vectra. Different thermal histories and clamping

*Corresponding author. Tel.: +46-8-7907640; fax: +46-8-7906946.

PII S0040-6031(98)00407-9

procedures were applied to Vectra samples to see how these factors affected the heating thermograms and the melting/crystallization behaviour.

Vectra is random copolymer and at high temperatures it forms a nematic mesophase. At lower temperatures, it crystallizes which is indeed remarkable in view of its random copolymer chain structure. The X-ray diffraction patterns reported by Gutierrez et al. [4] showed the presence of aperiodic meridional Bragg reflections as would be expected from a truly random distribution of the two comonomers. Windle et al. [5] suggested that the three-dimensional order indicated by the Bragg reflections may be explained by the presence of so-called non-periodic layer crystallites. Biswas and Blackwell [6] on the other proposed a model of truly random chains with essentially no lateral (inter-chain) comonomer register.

Sarlin and Törmälä [7,8] studied Vectra fibres and reported a melting range between 200 and 290°C and a melting enthalpy close to 5 J/g. A narrower and more distinct melting peak was observed in the second heating run. A series of heating thermograms of considerable variation in shape of 'noisy' character were displayed in the papers of Sarlin and Törmälä [7,8]. The lack of reproducibility of the melting traces – both in peak temperatures, melting enthalpies and general shape was evident. Annealing of Vectra at temperatures above 230°C resulted in an increased lateral order [9,10]. Furthermore, the low-temperature hexagonal crystal structure was transformed into an orthorhombic crystal structure [9,10]. Annealing of the nematic melt, above the crystal melting temperature has also been shown to lead to recrystallization [11,12]. It was proposed that the new crystals, with melting points 20–40°C higher than that of the virgin crystals, consisted of long sequences rich in hydroxybenzonic acid. Annealing in the solid state, below the crystal melting temperature has also been reported to give an increased molar mass resulting from transesterification reactions between chain ends [13–15]. Similar results were obtained for the same polymer in the nematic state [14].

2. Experimental

Vectra A950 (Hoechst-Celenese) used, in this study, is a thermotropic copolyester based on 73 mol% *p*-hydroxybenzonic acid and 27 mol% 2-hydroxy-6-naphthoic acid. Oriented dumbbell-shaped specimens were obtained by injection moulding. Details about the injection moulding have been described in Ref. [16]. The samples for the annealing experiments were prepared by microtoming 100-μm thick sections at different depths through the cross section using a Leica autocut microtome. Samples with no global orientation were prepared by compression moulding of carefully dried (100°C under vacuum) Vectra pellets at 320°C. The intensity profile of the X-ray diffraction pattern was for the compression moulded samples independent of azimuthal angle which confirmed the isotropic character of the films.

The thermal analysis was made with a Mettler DSC-820 equipped with a sample robot and temperature and energy calibrated with indium and tin. Isothermal annealing experiments for different periods of time, between 6 s and 3 h were performed at 250, 290 and 300°C. After annealing, the sample was heated by 20°C min to 360°C to reveal any formation of high-temperature melting crystals. Some samples were cooled to 50°C and, finally, heated by 20°C/min to 360°C after annealing. The samples used in all DSC work were circular shaped with a diameter of 3 mm and weighing 3–6 mg. The samples fitted exactly in the aluminium pans which facilitated the detection of shrinkage of sample during heating. All samples were taken out of the aluminium pan after the heat treatment and examined to reveal dimensional changes and the extent to which the sample had adhered to the pan. Different ways of placing the sample in the aluminium pan were tried: (a) direct contact of sample with the bottom of the pan; (b) immersion of sample in silicone oil; (c) placing the sample between two 10-μm thick Kapton films; (d) placing the sample between two thin foils of indium; and (e) placing the sample in the pan with a metallic disc compressing the sample to the bottom of the pan and preventing it from shrinking.

X-ray diffraction patterns were obtained by a Statton camera using CuK_α radiation (λ=0.154 nm) from a Philips PW 1830 generator. The Hermans orientation function (f) was calculated from the azimuthal angle intensity distribution of the equatorial Bragg reflection at $2\theta \approx 19.5^\circ$ ($d \approx 0.45$ nm) [16]. The director was defined as being parallel to the melt flow direction. The X-ray intensities were evaluated using an Image Analysis System Northern Light Model B90 light

table, Dage MTI 70 series camera, DTK 486-33 MHz PC, software by Optimas Bioscan. UN-Scorpion VGA framegrabber. Luminance was converted to intensity by calibrating with a photographic step tablet (Kodak No. 2).

3. Results and discussion

3.1. Constant rate heating of as-received samples

Samples continuously heated by 20°C min from room temperature to well above the crystal-nematic transition (360°C), generally, showed very dissimilar melting endotherms also when given the same thermal surrounding (Fig. 1). The thermograms displayed in Fig. 1 originates from samples in direct contact with the bottom of aluminium pan. The samples with the highest initial degree of orientation ($f \approx 0.5$) showed heating thermograms that were least reproducible. At temperatures above 200°C, when the chains started to gain mobility, the heating thermograms became noisy (Fig. 1). The crystal melting endotherm which appeared in the 260–290°C range was in some cases following directly after an 'exotherm' (Fig. 1). However, this low-temperature exothermal peak was not present in the thermograms of the samples immersed in silicone oil (Fig. 2). The results thus indicate that the exothermal peak is artificial and not due to a true physical exothermal process.

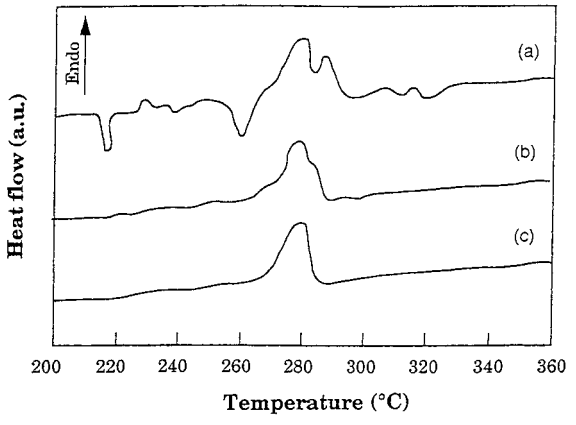

Fig. 1. Melting thermograms of samples with different degree of orientation placed directly in the DSC pan: (a) f=0.5; (b) f=0.2; and (c) f=0.0.

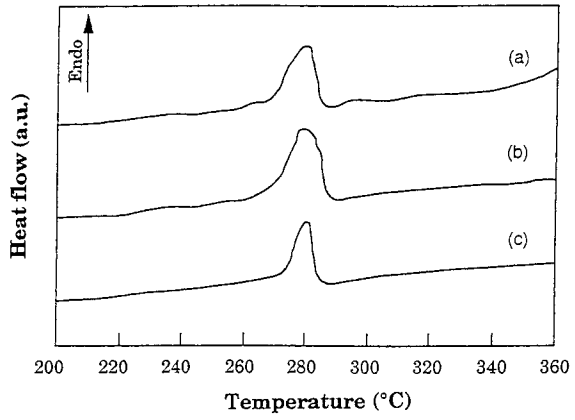

Fig. 2. Melting thermograms of samples with different degree of orientation immersed in silicone oil placed in the DSC pan: (a) f=0.5; (b) f=0.2; and (c) f=0.0.

Examination of the highly oriented samples ($f \sim 0.5$), placed in aluminium pans without lid, during heating on a heating plate revealed that the samples curled at 200–220°C leading to a loss of thermal contact. This substantiates the suggestion that noisy thermal signals prior to the melting region are due to thermally induced motions. Furthermore, the bimodal endothermal peak that was displayed in the thermograms of the 'unlubricated pans' (Fig. 1) and that was absent in the thermograms of the silicone-oil-immersed samples (Fig. 2) must also be due to thermally induced motion, causing a temporary loss of thermal contact. The samples with the lower initial degree of orientation ($f \sim 0.2$ and $f \sim 0$) exhibited relatively smooth thermograms and a less pronounced bimodality in the melting trace also for the samples in direct contact with the aluminium pan (Fig. 1). These samples showed only weak signs of curling during heating and they retained essentially their original dimensions after the heat treatment. The silicone-oil-immersed samples showed perfectly smooth thermograms with little or no bimodality in the melting peak between 260 and 290°C (Fig. 2). The conclusion that can be drawn is the 'true' melting process occurring within the 260–290°C range is unimodal.

Further, heating above the main melting temperature range (260–290°C) revealed in many cases a small high-temperature endothermal peak (0.15 ± 0.10 J/g) between 300 and 320°C. The more

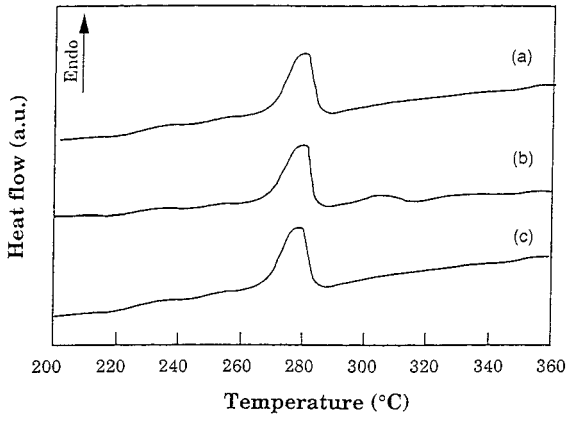

Fig. 3. Melting thermograms of samples with different degree of orientation placed between Kapton films in the DSC pan: (a) f=0.5; (b) f=0.2; and (c) f=0.0.

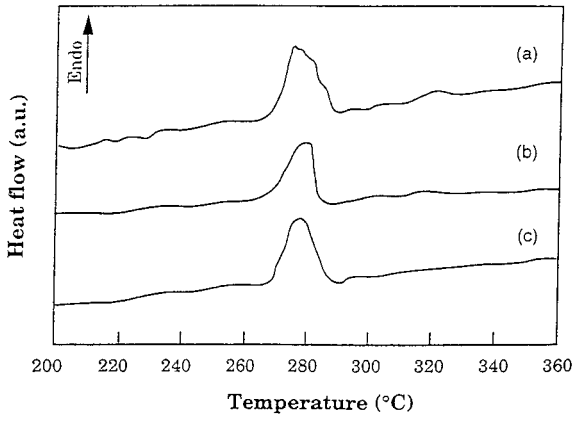

Fig. 4. Melting thermograms of samples with different degree of orientation constrained by a metal disc in the DSC pan: (a) f=0.5; (b) f=0.2; and (c) f=0.0.

noisy baseline for the samples in direct contact with the aluminium pan made it occasionally impossible to detect this tiny endothermal peak. It is clearly possible that the high-temperature peak is due to melting of PHBA-rich crystallites [11,12].

Fig. 3 shows heating thermograms for samples kept between Kapton films and, indeed, they resemble the thermograms of the oil-immersed samples (Fig. 2). The conditions prevailing for the oil-immersed samples, completely free shrinkage during heating were also prevailing for the Kapton-sandwiched samples. The free shrinkage conditions favour relaxation of orientation [3]. The constrained samples (by the insert of a metal disc which inhibits shrinkage during heating) exhibited noise-free heating thermograms with a mainly unimodal melting in the 260–290°C range (Fig. 4). The melting enthalpy (first heating) and the crystallization enthalpy (first cooling) was higher for constrained highly oriented (f∼0.5) samples than for the corresponding samples that were allowed to shrink freely (Fig. 5). The unoriented samples showed the same melting and crystallization enthalpies independent of degree of constraint.

The glass-transition temperature (T_g) was for the highly oriented samples (f∼0.5) dependent on the clamping procedure (Fig. 5). More constrained samples showed a lower T_g. This is not due to differences in heat transfer and thermal lag among the different samples; the positions of the melting and crystallization transitions was not influenced by the clamping

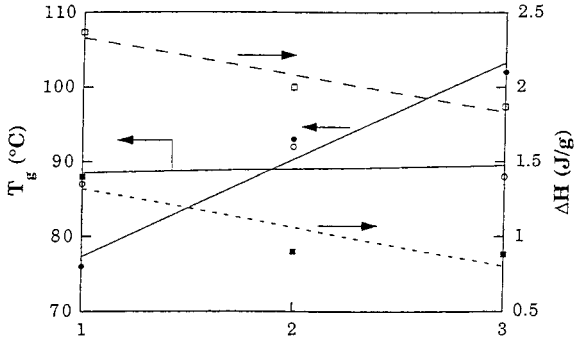

Fig. 5. The effect of clamping procedure on the glass-transition temperature and melting/crystallization enthalpy: (1) Metallic disc; (2) Direct in the DSC pan; (3) Kapton films; (●) T_g-skin-f=0.5 ; (○) T_g-core-f=0.2 ; (■) $\Delta H_{melting}$; (□) ΔH_{cryst}.

method. For the low-oriented samples (f∼0.2), the recorded glass-transition temperature was not influenced by the clamping procedure (Fig. 5).

The samples that were placed between thin indium foils had excellent thermal contact during and obtained thermograms were essentially noise free. These samples were able to shrink and in fact the sample shrinkage became even more extensive than for the oil-immersed samples.

3.2. The effect of heating and cooling cycles

The highly oriented samples (f∼0.5) showed a smaller melting enthalpy (first heating) than the crys-

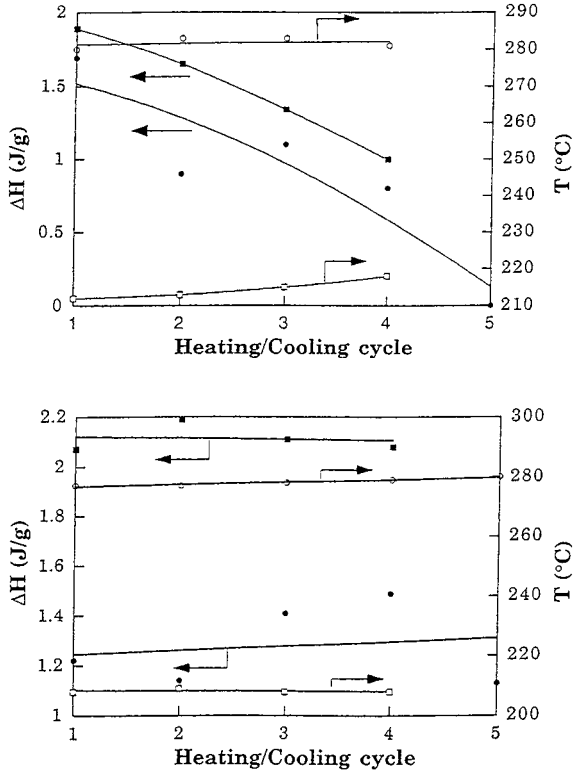

Fig. 6. The evolution of melting/crystallization enthalpies and temperatures on samples cycled five times between 50 and 360°C (20°C/min); (a) skin material (f=0.5): (●) $\Delta H_{melting}$; (■) ΔH_{cryst}; (○) T_m; (□) T_c; (b) Compression moulded film (f=0): (●) $\Delta H_{melting}$; (■) ΔH_{cryst}; (○) T_m; (□) T_c.

tallization enthalpy on the subsequent cooling (first cooling). It may be argued that the internal stresses resulting from the rapid cooling prevailing during the final stage of the injection moulding increases the energy of the system and, hence the enthalpy change during the first heating scan includes both the endothermal melting enthalpy and the exothermal relaxation of the internal stresses.

Fig. 6 shows melting/crystallization temperatures, and melting and crystallization enthalpies for oriented (f∼0.5) and isotropic samples (f∼0.0) ramped five times between 50 and 360°C up and down at the rate 20°C/min. The melting enthalpy decreased monotonically with the number of heating scans for the oriented material and the glass-transition temperature decreased from 95 to 88°C. No melting peak was seen in the fifth heating scan although the sample was checked to be in good thermal contact with the pan. The sample with no orientation was thermoreversible and displayed constant heats of fusion and melting temperatures for all heating cycles. It may be suggested that the steady decreasing melting enthalpy, melting peak temperature and glass-transition temperature with the number of heating/cooling cycles may all be due to thermal degradation of the polymer. If this assumption is true, it is difficult to find a good explanation to why degradation only occurred for the oriented sample and not for isotropic sample.

The oriented samples (f∼0.5) were annealed at 290°C for 60 min, cooled at rate of 20°C/min to 40°C, heated (20°C/min) to 360°C while recording, cooled down again to 40°C and, finally, reheated to 360°C by 20°C/min while recording the heating thermogram. The sample that was constrained with a metal disc in the pan showed a comparatively high melting enthalpy in the final heating stage (1 J/g) compared to the 0.2 J/g obtained for a sample allowed to shrink freely (Kapton-sandwiched sample). These data indicate that crystallization is enhanced by global orientation.

3.3. Annealing

Fig. 7 shows melting temperatures and heats of fusion for the highly oriented sample (f∼0.15) and isotropic sample (f=0.0) annealed at 250°C. The melting enthalpies for the oriented samples increase from 0.3 to 1 J/g after a short time of annealing to

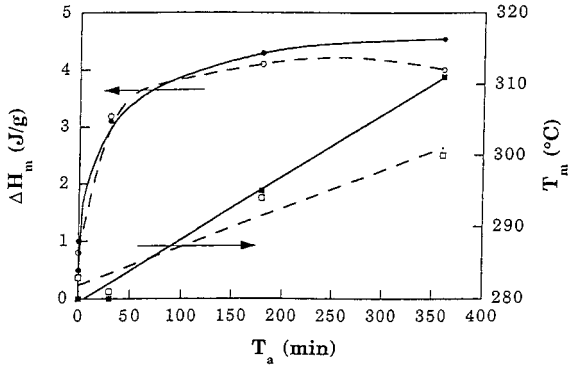

Fig. 7. Melting temperature and heats of fusion for samples annealed at 250°C. Skin material, f=0.5: (●) $\Delta H_{melting}$; (■) T_m; Unoriented material, f=0.0: (○) $\Delta H_{melting}$; (□) T_m.

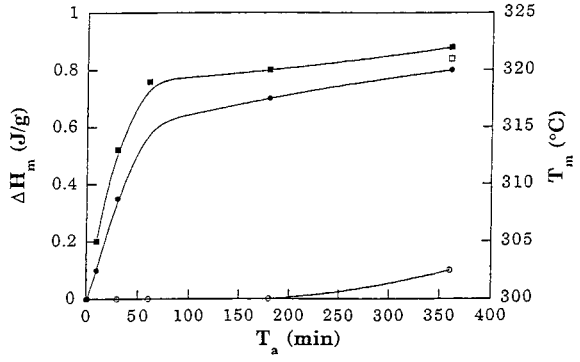

Fig. 8. Melting temperatures and heats of fusion for samples annealed at 290°C. Skin material, f=0.5: (●) $\Delta H_{melting}$; (■) T_m; Unoriented material, f=0.0: (○) $\Delta H_{melting}$; (□) T_m.

~4.5 J/g after 6 h annealing. This was accompanied by an increase in melting temperature from 280 to 311°C. The melting peak after 10 min of annealing was broad and diffuse. Further annealing led to a narrowing of the melting and the integration of the melting enthalpy was simplified. The isotropic samples showed on annealing a similar increase in the melting enthalpy and a slightly smaller increase in the melting peak temperature (Fig. 7). Some of the annealed isotropic samples exhibited multimodal melting.

Fig. 8 shows the behaviour of the highly oriented (f~0.5) and the isotropic samples (f~0.0) after annealing at 290°C. This temperature is just above the melting region. The occurrence of a recrystallization process is obvious after 10 min of annealing of the oriented sample (f~0.5), demonstrated by the tiny (0.1 J/g) endotherm at 305°C. Both the melting enthalpy and the melting peak temperature increased with the annealing time, approaching the values 0.8 J/g and 322°C, respectively, after 6 h of annealing. The recrystallization was principally the same for the samples with f~0.2 (not shown in any figure). The recrystallization of the globally isotropic films was however considerably slower; after 6 h of annealing the melting enthalpy was 0.1 J/g. The melting peak temperature for the annealed isotropic sample was however the same as for the oriented sample (322°C). Samples placed between Kapton sheets or immersed in silicone oil gave basically the same results as for samples with direct metallic contact. However, the use of Kapton or silicone-oil-immersion is advantageous because the thermograms become smoother with less noise.

The recrystallization rate at 300°C was very slow. Melting enthalpies after 6 h annealing were ca. 0.1–0.5 J/g, independent of the degree of orientation, and the melting peak temperature was between 330 and 355°C.

4. Conclusions

Evaluation of DSC thermograms of oriented liquid crystalline polymers is very difficult. The oriented samples are at elevated temperatures in constant motion due to retraction of the oriented molecules, resulting in temporary loss of thermal contact and irreproducible DSC thermograms. Samples immersed in silicone oil or surrounded by Kapton films are free to shrink, in good thermal contact with the aluminium pan and the heating thermograms are essentially noise-free and artificial endothermal or exothermal peaks which are otherwise seen are absent. Samples clamped with a metal disc did not shrink on heating and the thermograms were smooth without artificial peaks. Annealing of Vectra samples between 250 and 300°C led to a gradual increase in both the melting enthalpy and the melting peak temperature with increasing annealing time. Crystallization of the pure nematic polymer was facilitated by orientation.

Acknowledgements

This study has been sponsored by the Swedish Research Council of Engineering Sciences (TFR; grant 91-245), the Swedish Natural Research Council (NFR; grant K-KU 1910-300) and the Royal Institute of Technology.

References

[1] M.J. Richardson, Compreh. Polym. Sci. 1 (1989) 867.
[2] N. Billon, J.M. Haudin, J. Thermal Anal. 42 (1993) 679.
[3] G. Wiberg, U.W. Gedde, Polymer 38 (1997) 3753.
[4] G. A Gutierrez, R.A. Chivers, J. Blackwell, J.B. Stomatoff, H. Yoon, Polymer 24 (1983) 937.
[5] A.H. Windle, C. Viney, R. Golombeck, A.M. Donald, D.R. Mitchell, Faraday Discussion Chem. Soc. 79 (1985) 55.

[6] A. Biswas, J. Blackwell, Macromolecules 21 (1988) 3146.
[7] J. Sarlin, P. Törmälä Polymer Commun. 31 (1990) 372.
[8] J. Sarlin, P. Törmälä Polym. Eng. Sci. 29 (1991) 395.
[9] A. Kaito, M. Kyotani, K. Nakayama, Macromolecules 24 (1991) 3244.
[10] D.J. Wilson, C.G. Vonk, A.H. Windle, Polymer 34 (1993) 227.
[11] Y.G. Lin, H.H. Winter, Macromolecules 21 (1988) 2439.
[12] Y.G. Lin, H.H. Winter, Macromolecules 24 (1991) 2877.
[13] J. Economy, R.D. Johnson, J.R. Lyerla, A. Mühlebach, Liquid Crystalline Polymers, Chap. 10, ACS Symposium series 435, 1990.
[14] A. Mühlebach, J. Economy, R.D. Johnson, T. Karis, J.R. Lyerla, Macromolecules 23 (1990) 1803.
[15] S.B. Warner, J. Lee, J. Polym. Sci. Polym. Phys. Ed. 32 (1994) 1759.
[16] K. Engberg, U.W. Gedde, Progr. Colloid Polym. Sci. 87 (1992) 57.